One-pot synthesis of efficient multifunctional nitrogen doping carbon dots with efficient yellow fluorescent emission for detection of hypochlorite and thiosulfate

Yifang Gao[a], Yang Liu[b], Huilin Zhang[b], Wenjing Lu[b], Yuan Jiao[a]*,

Shaomin Shuang[b] and Chuan Dong[b]*

Experimental

Determination of QY

The quantum yield Φs of the NCDs were determined by a comparative method as follows:

$$\Phi_S = \Phi_R (Grad_S/Grad_R)(\eta_S{}^2/\eta_R{}^2)$$

where Grad is the gradient from the plot of integrated fluorescence intensity against absorbance and η ((1.33 for water and 1.36 for ethanol) is the refractive index of the solvent. The subscripts S and R represent NCDs and the reference (rhodamine 6G in ethanol). To prevent the re-absorption effect, the absorbances of NCDs and quinine sulfate solutions in the 10-mm fluorescence cuvette were adjusted to less than 0.10 at the excitation wavelength (λex) of 380 nm (i.e., the absorption maximum of NCDs). The integrated fluorescence intensity was the area under the PL curve in the wavelength range 400–700 nm. The Φ_R was taken as 0.95 since it is almost independent (within 5%) with λex at 200–400 nm.

Table S1. Elemental analysis of the as-synthesised NCDs.

Sample name	Elemental content (%)			
	C	H	N	O (Calculated)
NCDs	30.7	6.2	15.2	47.9

Table S2. Lifetime calculations from the time-resolved decay profiles of NCDs, NCDs-ClO$^-$ and NCDs-ClO$^-$-S$_2$O$_3{}^{2-}$.

Sample	τ1 (ns)	Percentage (%)	τ2 (ns)	Percentage (%)	Ave.τ (ns)
NCDs	4.3242	87.77	11.5887	12.23	5.21
NCDs-ClO$^-$	4.0247	82.16	9.3701	17.84	4.98
NCDs-ClO$^-$-S$_2$O$_3{}^{2-}$	4.2956	89.31	12.5201	10.69	5.17

Table S3. Comparison of detection limit between the proposed fluorescent sensor and other reported detection methods for ClO$^-$.

Sensing probe	Response region	Detection limits	Reference
CDs–rhodamine B	10–140 μM	4 μM	[1]
Graphene quantum dots	0.5–1.0 μM	0.3 μM	[2]
CDs	5–200/2.5–50μM	2.0/0.5 μM	[3]

Ethanol-derived CDs	0.1-2 µM	100 nM	4
N-doped CDs	0.1–27 µM	0.0297 µM	5
MF-CDs	0.6–20 µM	0.18 µM	6
NCDs	0.067–19.33/24–98 µM	0.013 µM.	This work

Table S4. Comparison of detection limit between the proposed fluorescent sensor and other reported detection methods for PPi.

Sensing probe	Response region	Detection limits	Reference
N-doped CDs	1-20/20–80 µM	1.17 µM	7
C-dots/Fe^{3+}	/	8.47 µM	8
NCDs	6.6-100 µM	0.78 µM	This work

Table S5. Application of the proposed fluorescence (FL) method for the determination of ClO^- in tap water sample spiked with different amounts of ClO^-.

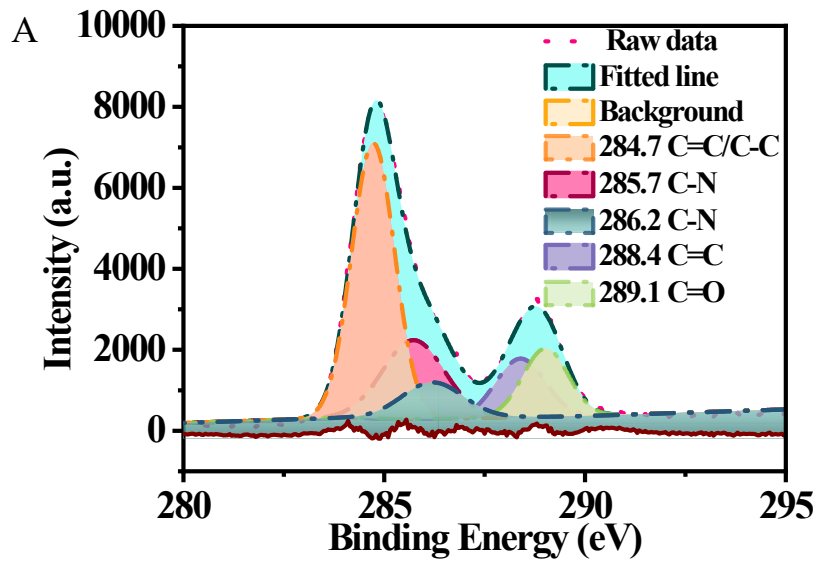| Sample	The FL method			
	Added	Found	Recovery	R.S.D.
	(µM)	(µM)	(%)	(%)
1	5	4.86	97.2	2.1
1	20	20.2	100.1	3.2
2	50	48.8	97.6	2.4
3	80	80.1	100.1	3.1
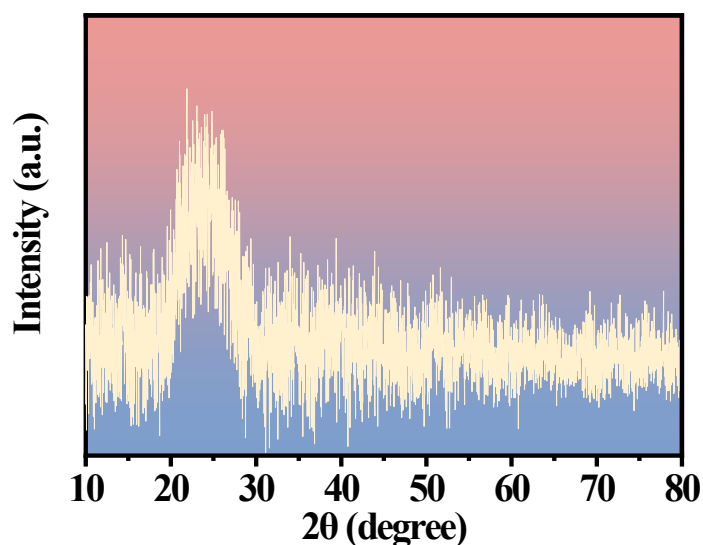
Figure S1 X-ray diffraction (XRD) pattern of the NCDs.
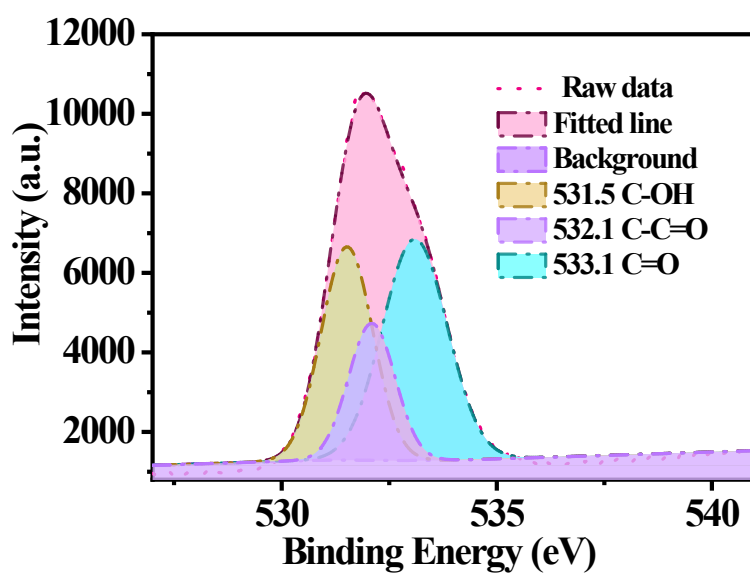
A

B
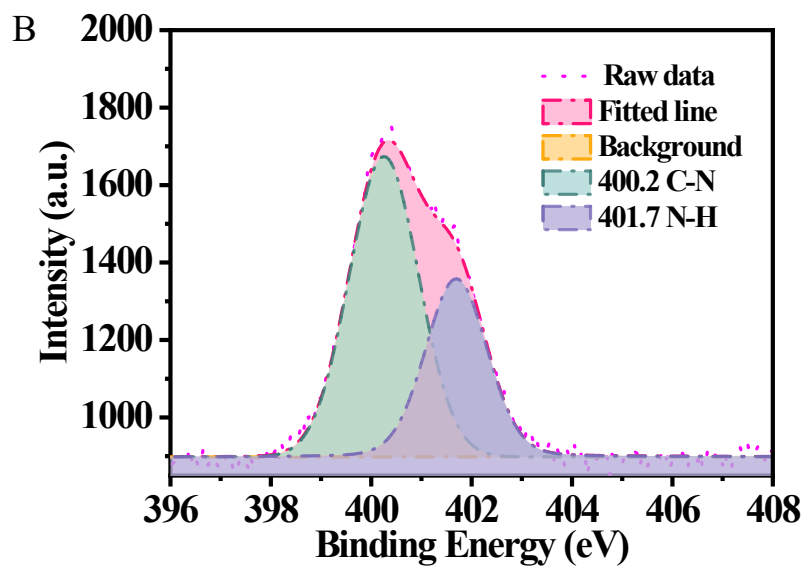
C

Figure S2 High-resolution XPS data of C 1s (A), N 1s (B) and O1s (C) of NCDs.
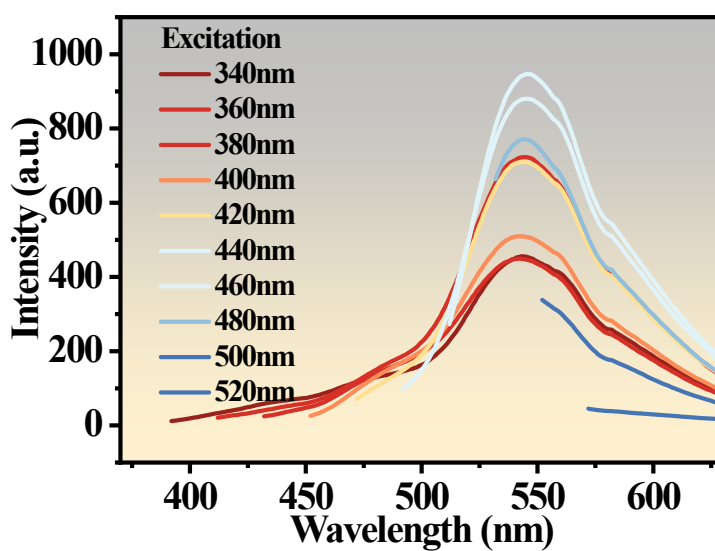

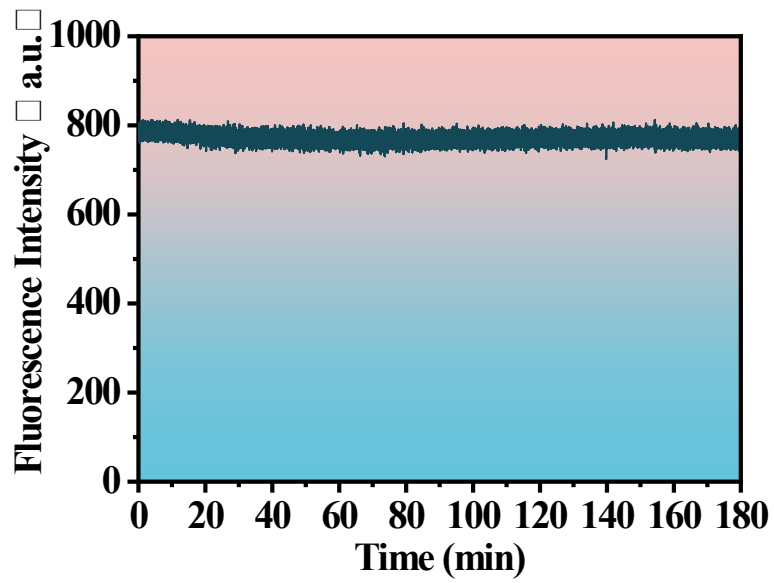**Figure S3** FL emission spectra of the NCDs under different excitation wavelengths.

Figure S4 Effect of time intervals of irradiation with xenon arc light on fluorescence intensity of NCDs.
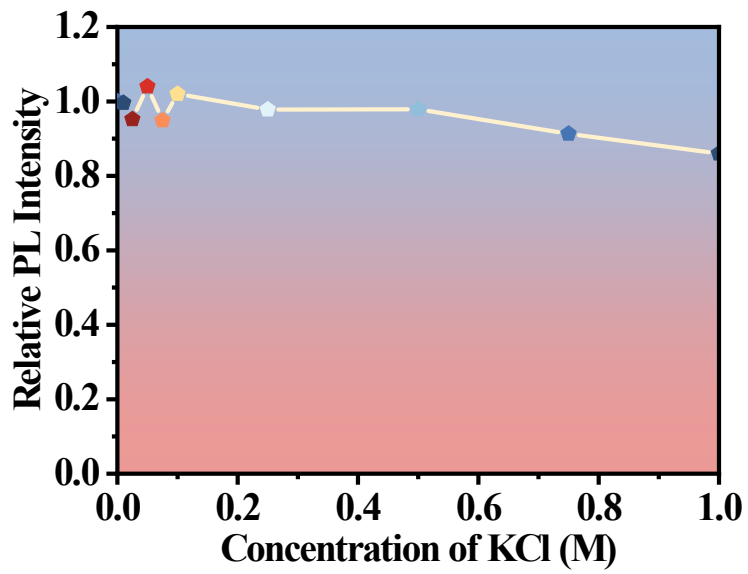

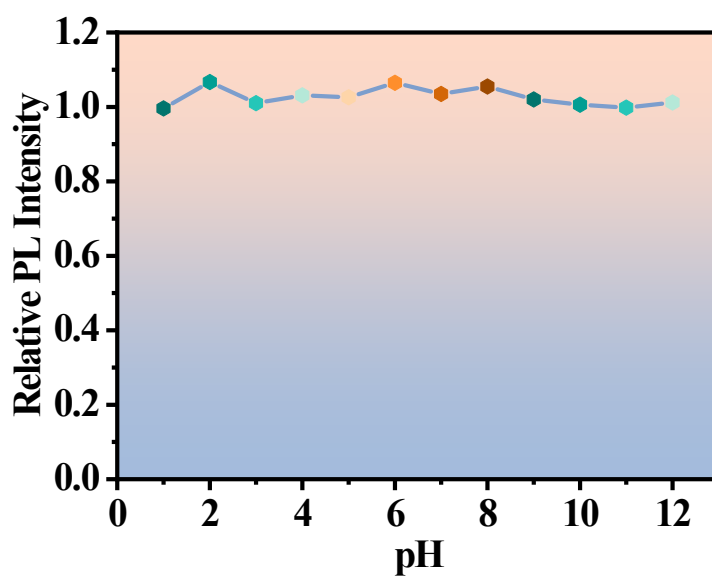**Figure S5** Effect of ionic strength on fluorescence intensity of NCDs.

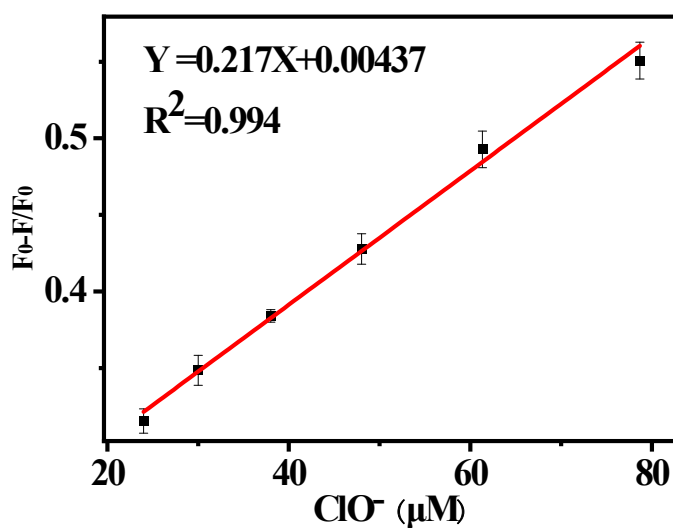**Figure S6** Effect of pH on FL intensity of NCDs. The pH is adjusted by the PBS buffers.

$Y = 0.217X + 0.00437$

$R^2 = 0.994$

Figure S7 A linear plot showing the relationship between the FL intensity and the concentrations of ClO$^-$ (λex =378 nm).
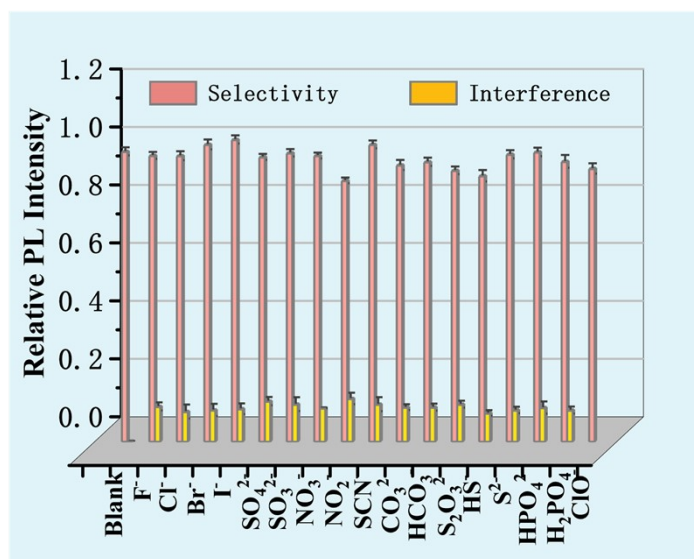
Figure S8 The influence of different metal ions on the fluorescence of NCDs.
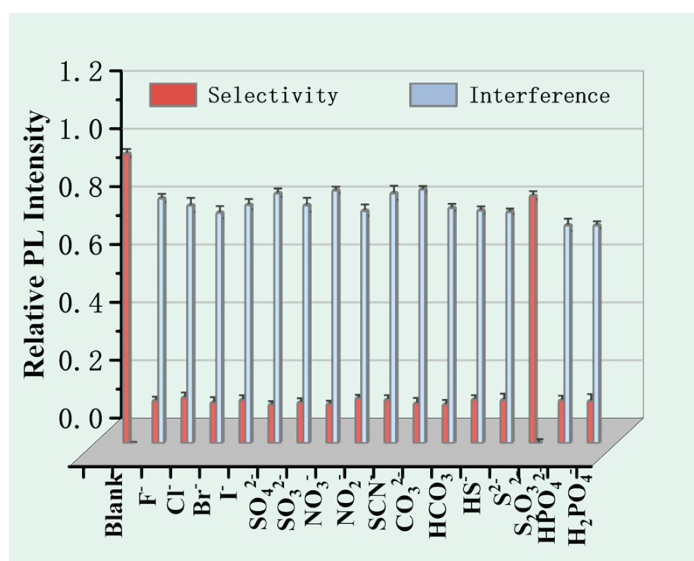

Figure S9 The influence of different different anion on the fluorescence of NCDs-ClO⁻.
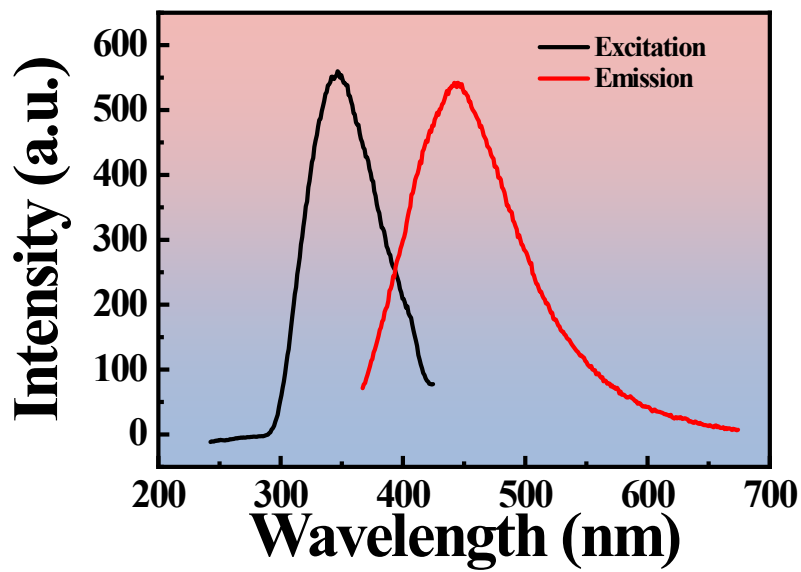
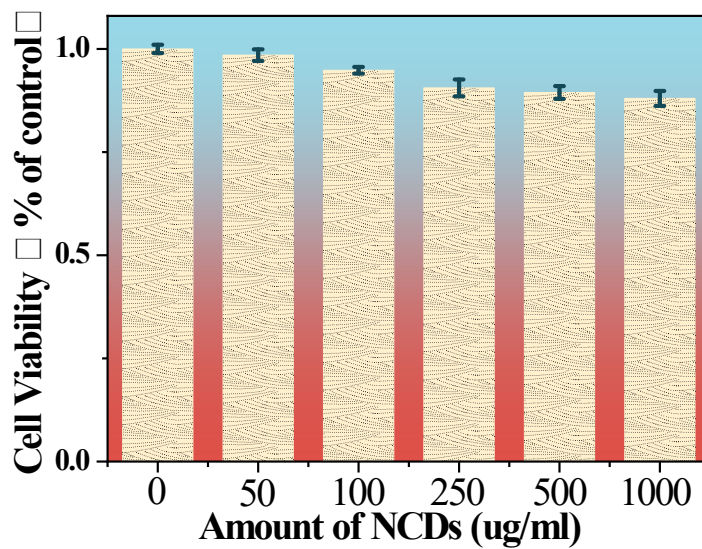**Figure S10** The FL spectra of the NCDs synthesized from citric acid alone.

Figure S11 Cytotoxicity testing results of NCDs on SMMC7721cells viability. The values representpercentage cell viability (mean% ± SD, n=6).
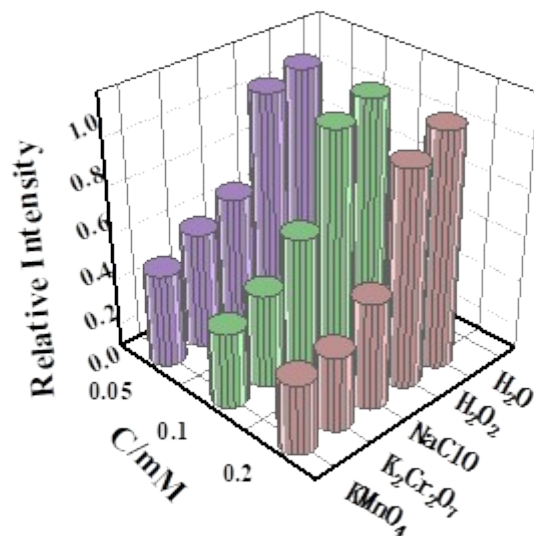
Figure S12 Fluorescence response of 200 μg mL^{-1} N-CDs in the presence of different oxidants (H_2O_2, $NaClO_3$, $KMnO_4$ and $K_2Cr_2O_7$).

1. Ding, Y.; Ling, J.; Cai, J.; Wang, S.; Li, X.; Yang, M.; Zha, L.; Yan, J., A carbon dot-based hybrid fluorescent sensor for detecting free chlorine in water medium. *Analytical Methods* **2016,** *8* (5), 1157-1161.

2. Hallaj, T.; Amjadi, M.; Manzoori, J. L.; Shokri, R., Chemiluminescence reaction of glucose-derived graphene quantum dots with hypochlorite, and its application to the determination of free chlorine. *Microchimica Acta* **2015,** *182* (3), 789-796.

3. Simões, E. F. C.; Leitão, J. M. M.; da Silva, J. C. G. E., Carbon dots prepared from citric acid and urea as fluorescent probes for hypochlorite and peroxynitrite. *Microchimica Acta* **2016,** *183* (5), 1769-1777.

4. Hu, Y.; Yang, J.; Jia, L.; Yu, J.-S., Ethanol in aqueous hydrogen peroxide solution: Hydrothermal synthesis of highly photoluminescent carbon dots as multifunctional nanosensors. *Carbon* **2015,** *93*, 999-1007.

5. Lin, Y.; Yao, B.; Huang, T.; Zhang, S.; Cao, X.; Weng, W., Selective determination of free dissolved chlorine using nitrogen-doped carbon dots as a fluorescent probe. *Microchimica Acta* **2016,** *183* (7), 2221-2227.

6. Zhan, Y.; Luo, F.; Guo, L.; Qiu, B.; Lin, Y.; Li, J.; Chen, G.; Lin, Z., Preparation of an Efficient Ratiometric Fluorescent Nanoprobe (m-CDs@[Ru(bpy)3]2+) for Visual and Specific Detection of Hypochlorite on Site and in Living Cells. *ACS Sensors* **2017,** *2* (11), 1684-1691.

7. Wang, B.; Tan, H.; Zhang, T.; Duan, W.; Zhu, Y., Hydrothermal synthesis of N-doped carbon dots from an ethanolamine–ionic liquid gel to construct label-free multifunctional fluorescent probes for Hg2+, Cu2+ and S2O32−. *Analyst* **2019,** *144* (9), 3013-3022.

8. Dhenadhayalan, N.; Lin, K.-C., Chemically Induced Fluorescence Switching of Carbon-Dots and Its Multiple Logic Gate Implementation. *Scientific Reports* **2015,** *5* (1), 10012.